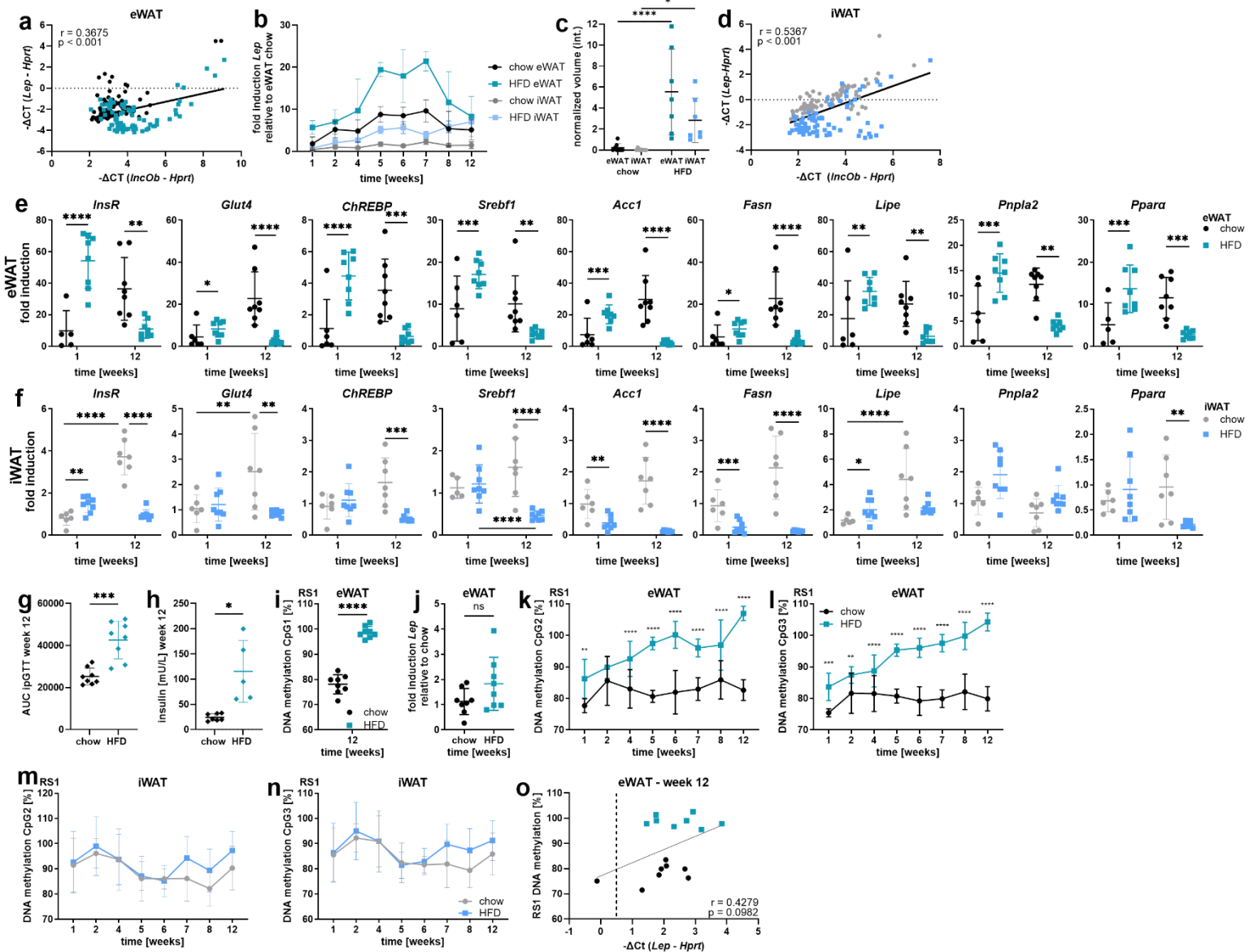


## **Supplemental information**

### **A Novel mechanism for depot-specific leptin gene expression regulation and its persistence after weight loss**

**Natalie Taege, Jan Hendric Britsemmer, Andreas Israel, Christin Krause, Sina Junge, Annette Feuchtinger, Siegfried Ussar, Paul Thomas Pfluger, Timo Gemoll, Sonja Charlotte Schriever, and Henriette Kirchner**



**Figure S1. Fat depot-specific RS1 DNA methylation and *IncOb* expression regulate *Lep* expression without altering glucose and lipid metabolism gene expression between the depots. Related to Figure 1.**

(a) eWAT: Pearson correlation of *Lep* expression ( $-\Delta\text{CT}(\text{Ct}(\text{Lep}) - \text{Ct}(\text{Hprt}))$ ) with *IncOb* expression ( $-\Delta\text{CT}(\text{Ct}(\text{IncOb}) - \text{Ct}(\text{Hprt}))$ ) in total DIO cohort.

(b) *Lep* expression in eWAT and iWAT of the DIO cohort over time, shown as fold induction relative to eWAT chow week 1.

(c) Leptin protein content in eWAT and iWAT (week 12) measured by immunoblotting; blots in Fig. S2. Data normalized to total protein and a calibrator.

(d) iWAT: Pearson correlation of *Lep* expression with *IncOb* expression in the total DIO cohort.

(e-f) Expression of *InsR*, *Glut4*, *ChREBP*, *Srebf1*, *Acc1*, *Fasn*, *Lipe*, *Pnpla2*, and *Ppara* in (e) eWAT and (f) iWAT at weeks 1 and 2, shown as fold induction relative to chow week 1.

(g) Intraperitoneal glucose tolerance test (ipGTT) in week 12 shown as area under the curve (AUC), data also published<sup>1</sup>.

(h) Plasma insulin concentration (mU/L) at sacrifice (week 12); data also published<sup>1</sup>.

(i-j) RS1 DNA methylation (i) and *Lep* expression relative to chow (j) in eWAT (week 12).

(k-n) RS1 DNA methylation at CpG2 and CpG3 in eWAT (k, l) and iWAT (m, n).

(o) Pearson correlation of *Lep* expression ( $-\Delta\text{CT}$  of  $\text{Ct}(\text{Lep}) - \text{Ct}(\text{Hprt})$ ) and RS1 DNA methylation in eWAT of DIO cohort, week 12.

Data are presented as mean  $\pm$  SD. Statistical analysis: Two-way repeated measures ANOVA with post hoc Fisher's LSD test (c), two-way ANOVA with Holm-Sidak post hoc test (e, f, k-n); two-tailed Welch's t-test (g, h); Student's t-test (i, j). Significance: \* $p < 0.05$ , \*\* $p < 0.01$ , \*\*\* $p < 0.001$ , \*\*\*\* $p < 0.0001$ . DIO, diet-induced obesity; eWAT, epididymal white adipose tissue; iWAT, inguinal white adipose tissue; HFD, high-fat diet; *IncOb*, long non-coding RNA Ob; genes: *Lep*, leptin; *Hprt*, hypoxanthine guanine phosphoribosyl transferase; *InsR*, insulin receptor; *Glut4*, glucose transporter type 4; *ChREBP*, carbohydrate-responsive element-binding protein; *Srebf1*, sterol regulatory element-binding transcription factor 1; *Acc1*, acetyl-CoA carboxylase alpha; *Fasn*, fatty acid synthase; *Lipe*, hormone-sensitive lipase; *Pnpla2*, patatin-like phospholipase domain-containing 2 (ATGL); *Ppara*, peroxisome proliferator-activated receptor alpha.

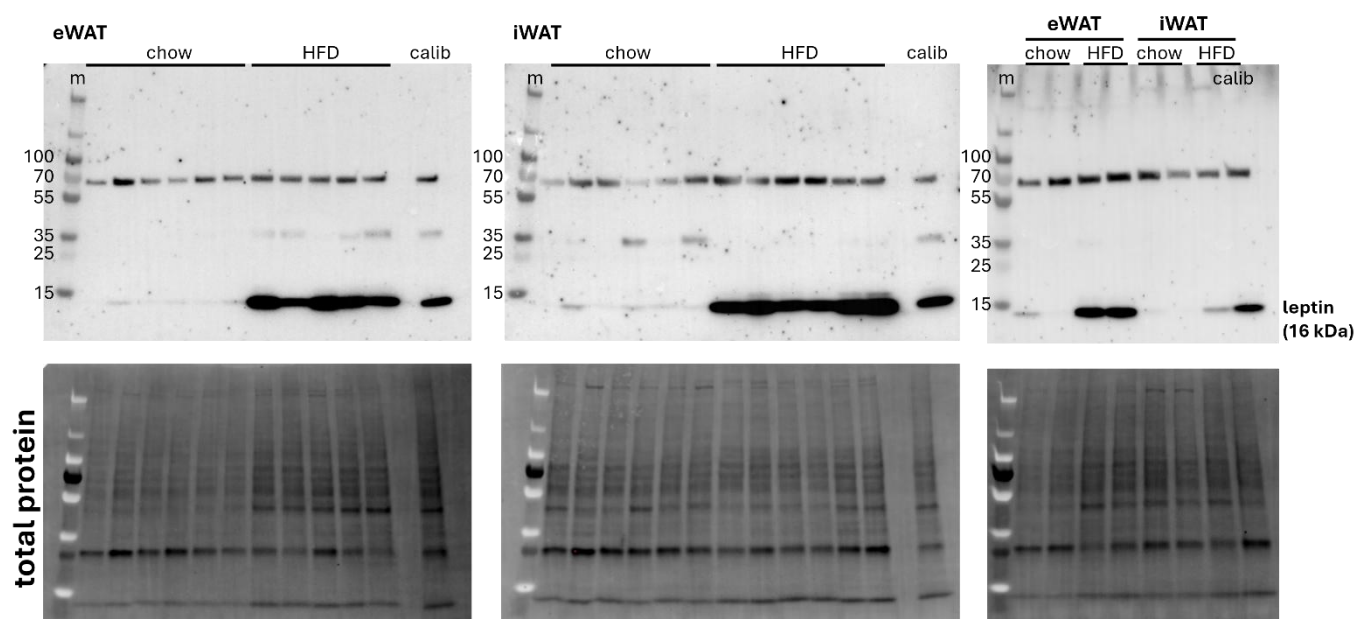


**Figure S2: Leptin protein levels are comparable between eWAT and iWAT at week 12 of DIO. Related to Figure S1 and STAR Methods.**

Immunoblots of eWAT and iWAT from 12-week HFD- or chow-fed mice. Upper panel: leptin antibody detection showing an unspecific band at ~70 kDa. Lower panel: total protein normalization (see blot). eWAT, epididymal white adipose tissue; iWAT, inguinal WAT; DIO, diet-induced obesity; HFD, high-fat diet; calib, calibrator.

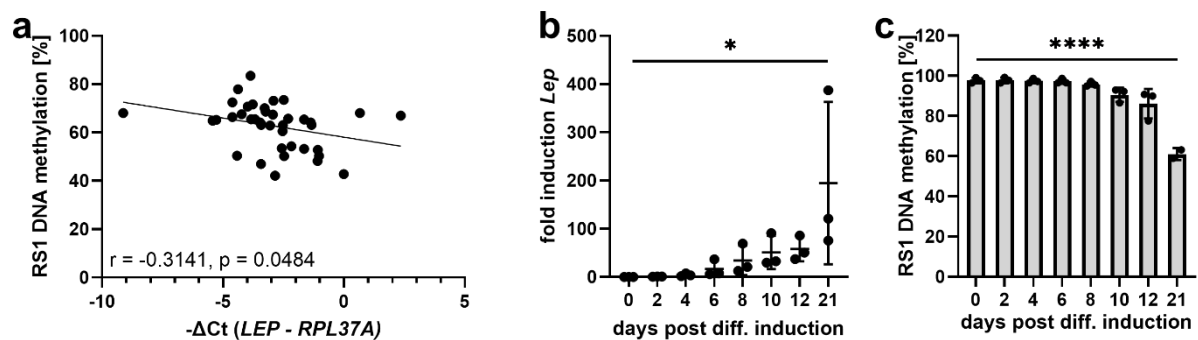


**Figure S3: RS1 DNA methylation inversely associates with *LEP* expression in human VAT and 3T3 adipocytes, supporting an inhibitory regulatory role. Related to Figure 2.**

(a) Pearson correlation of RS1 DNA methylation and *LEP* expression ( $-\Delta Ct$  of *Ct(LEP)* – *Ct(RPL37A)*) in human subjects with obesity (mean BMI =  $43.5 \pm 4.3$ ).

(b) *Lep* expression in differentiating 3T3-L1 adipocytes, relative to day 2 post differentiation (diff.) induction.

(c) RS1 DNA methylation in differentiating 3T3-L1 adipocytes, relative to day 2 post differentiation (diff.) induction.

Data are presented as mean  $\pm$  SD (b, c). Statistical analysis: One-way repeated measures ANOVA. Significance: \* $p < 0.05$ , \*\*\*\* $p < 0.0001$ .

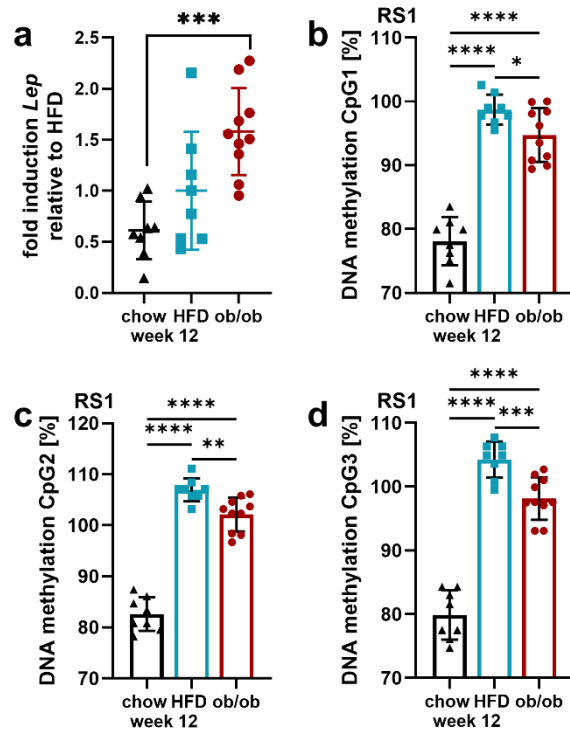


**Figure S4: Changes in RS1 DNA methylation in eWAT are independent of central leptin feedback signaling, related to Figure 3 and STAR Methods.**

(a) *Lep* expression and (b–d) RS1 DNA methylation in genetically obese *ob/ob* mice compared to 12-week HFD-fed mice and their chow-fed controls from the DIO cohort.

Data are presented as mean  $\pm$  SD. Statistical analysis: one-way ANOVA with Holm–Sidak post hoc test. Significance: \* $p < 0.05$ , \*\* $p < 0.01$ , \*\*\* $p < 0.001$ , \*\*\*\* $p < 0.0001$ . *LEP*, leptin gene; *RPL37A*, Ribosomal Protein L37a gene.

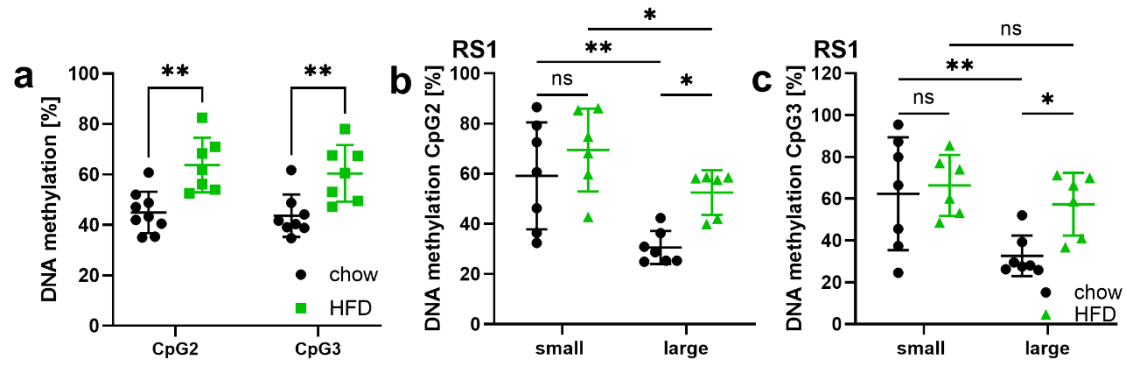


**Figure S5: DNA methylation results measured at additional RS1 CpG sites (CpG2 and CpG3) in sorted and size-stratified adipocytes. Related to Figure 3.**

(a) RS1 DNA methylation of the sorted adipocytes (Fig. 3).

(b, c) RS1 DNA methylation of size sorted adipocytes (Fig. 3).

Data are presented as mean  $\pm$  SD. Statistical analysis: (a) two-tailed Student's t-test for each CpG; (b, c) two-way repeated measures ANOVA with multiple comparison after Fisher's LSD. Significance: \* $p < 0.05$ , \*\* $p < 0.01$ , \*\*\* $p < 0.001$ , \*\*\*\* $p < 0.0001$ . *Lep*, leptin gene.

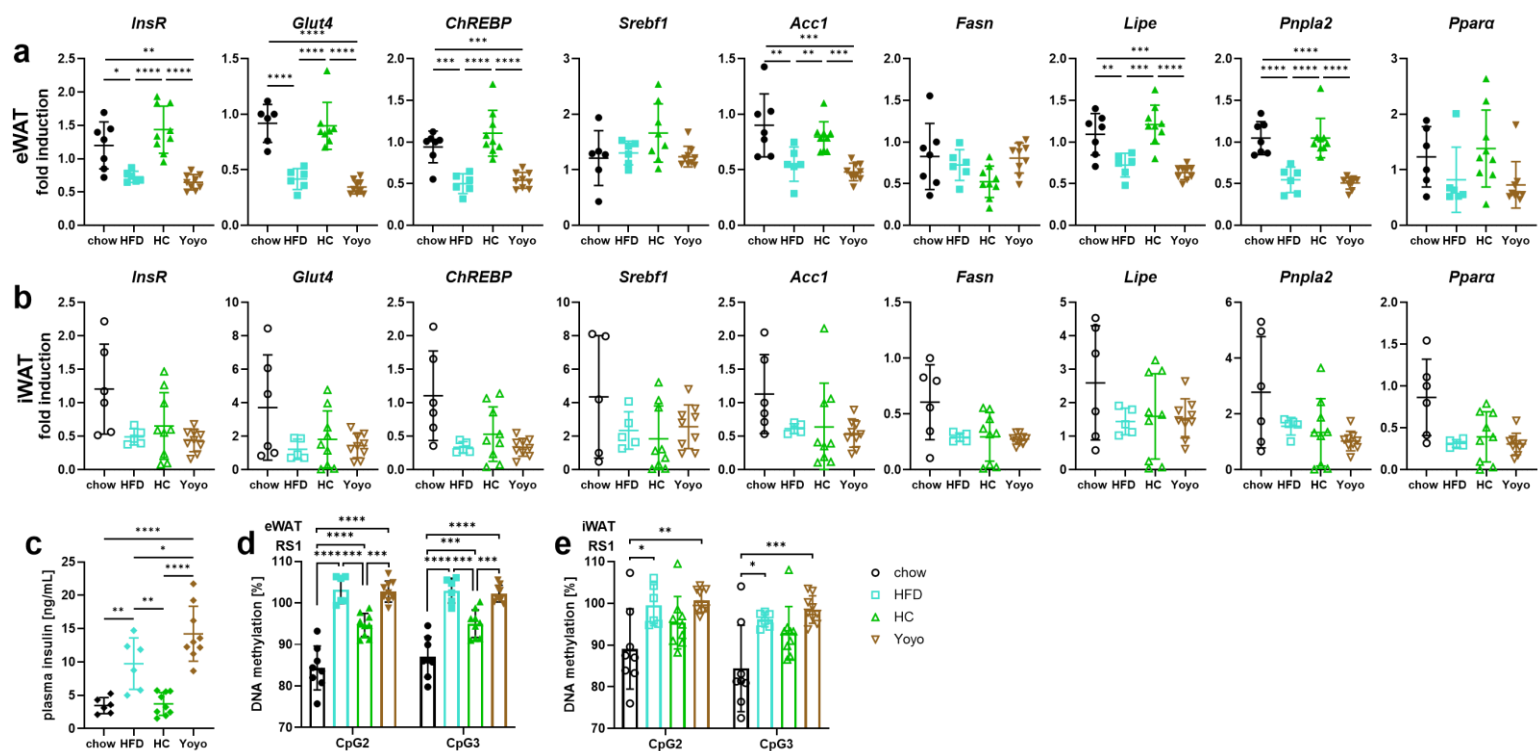


**Figure S6: Cycling of glucose and lipid metabolism genes in eWAT but not iWAT mirrors weight fluctuations and corresponds to plasma insulin levels. Related to Figure 4.**

(a-b) Expression of *InsR*, *Glut4*, *ChREBP*, *Srebf1*, *Acc1*, *Fasn*, *Lipe*, *Pnpla2*, and *Ppara* in (a) eWAT and (e) iWAT of the weight cycling cohort, shown as fold induction relative to chow.

(c) Plasma insulin levels [ng/mL] of weight cycling cohort, data published<sup>2</sup>.

(d-e) DNA methylation at additional CpG sites of RS1 in (d) eWAT and (e) iWAT.

Data are presented as mean  $\pm$  SD. Statistical analysis: One-way ANOVA with Tukey's multiple comparisons test. Significance: \*p<0.05, \*\*p<0.01, \*\*\*p<0.001, \*\*\*\*p<0.0001. eWAT, epididymal white adipose tissue; iWAT, inguinal white adipose tissue; HFD, high-fat diet; genes: *Lep*, leptin; *Hprt*, hypoxanthine guanine phosphoribosyl transferase; *InsR*, insulin receptor; *Glut4*, glucose transporter type 4; *ChREBP*, carbohydrate-responsive element-binding protein; *Srebf1*, sterol regulatory element-binding transcription factor 1; *Acc1*, acetyl-CoA carboxylase alpha; *Fasn*, fatty acid synthase; *Lipe*, hormone-sensitive lipase; *Pnpla2*, patatin-like phospholipase domain-containing 2 (ATGL); *Ppara*, peroxisome proliferator-activated receptor alpha.



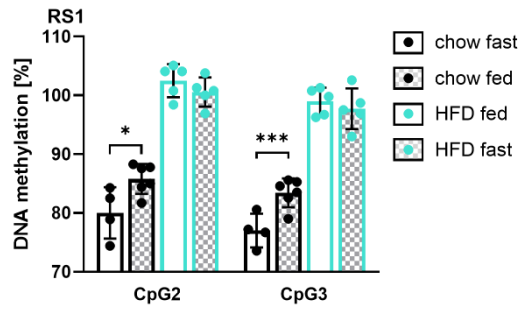


**Figure S7: DNA methylation at additional CpG sites of RS1 in eWAT of overnight fasted (16h) and fed chow or HFD-fed mice. Related to Figure 5.**

Data are presented as mean  $\pm$  SD. Data were analyzed using two-way ANOVA with Holm-Sidak post hoc test. Significance: \* $p < 0.05$ , \*\*\* $p < 0.001$ . Abbreviations: eWAT, epididymal white adipose tissue; HFD, high-fat diet.

Table S1: General settings of COPAS FP500 during adipocyte size sorting

FlowCell	500 micron	
Scan Rate	2500 K	
Focal point 1	Trigger channel	thresholds: T=5000 T1=5000 T2=2000
	Extinction	N1=300 N2=300 Dip=0 Pre-pad=0 Post-pad=0
Focal point 2	Trigger channel	thresholds: T=2000 T1=5000 T2=2000
	Extinction	N1=300 N2=300 Dip=0 Pre-pad=0 Post-pad=0
Minimum time of flight	60	
Channels set-up	Extinction	gains=2.0pmt volts=0
	Green	gains=1.3pmt volts=350
	Yellow	gains=1.0pmt volts=300
	Red	gains=1.5pmt volts=450
Pressure		2.000
		variable
		2.500
		3.000
		0.000
Drop width	6.0	
Sort Delay	9.0	
Coincidence mode	Enrichment	
Laser	Sapphire488	Power = 50
Buffer	1x PBS with 0.5 % BSA	

Table S2: Gating settings of COPAS FP500 for chow and/or HFD if indicated

red+ (red PH, green PH)	(523,64); (473,30); (560,8); (998,1); (1001,111); (642,100)
green+, chow (red PH, green PH)	(147,231); (180,92); (299,100); (456,143); (667,214); (704,251); (450,250)
green+, HFD (red PH, green PH)	(147,231); (118,80); (295,92); (456,143); (667,214); (704,251); (450,250)
unstained, chow (red PH; green PH)	(94,66); (118,1); (402,21); (487,76); (294,86)
unstained, HFD (red PH, green PH)	(92,59); (118,1); (402,21); (487,76); (103,60)
large, chow (TOF)	214.2 - 1024.0
large, HFD (TOF)	377.5 - 1020.1
intermediate, HFD (TOF)	214.2 - 365.7
small (TOF)	20.9 - 198.5

TOF = time of flight, PH=peak height

Table S3: CpG positions in genomic context of mouse of measured RS1 DNA methylation site.

Site	UCSC genome	Chromosome	Single CpG locations
RS1	mm10	chr.6	29032574, 29032582, 29032597

Table S4: Specific settings for scan range, ion mobility, and mass accuracy of mass spectrometry in diaPASEF mode with estimated cycle time of 1.8 s

Scan range	positive ion polarity	100-1700 m/z
TIMS setting	ion mobility range	0.6-1.6 1/K0
	ramp time	100 ms
	accumulation time	100 ms
	ramp rate	9.43 Hz
MS/MS setting	mass range	400 – 1201.0 Da
	mobility range	0.6-1.6 1/K0
fixed dia-PASEF window	width	26.0 Da
	mass overlap	1.0 Da
	mobility overlap	0.0 1/K0
mass steps	32	
mobility window/cycle	1.0	

Table S5: Specific settings for analysis with DIA-NN software (v1.8.1) using the human UniprotKB/swiss-prot database (downloaded on 12/22/2021) for deep learning based in silico spectral library generation.

LC mode	high precision
RT-dependent cross normalization	enabled
Library generation	smart profiling
neural network classifier	single pass mode
Mass & MS1 accuracy	10.0
scan window	0
Match between runs	enabled
protease setting	trypsin/P
missed cleavage acceptance	1.0
max no. of variable modifications	0.0
N-terminal methionine excision	enabled (fixed modification)
cysteine carbamidomethylation	enabled (fixed modification)
peptide length range	7-30
precursor charge range	2-4
precursor m/z range	100-1700
fragment ion m/z range	400-1201
'pg_matrix' (protein groups) output filter	1% FDR

[1] Geißler, C., Krause, C., Neumann, A.M., Britsemmer, J.H., Taege, N., Grohs, M., et al., 2022. Dietary induction of obesity and insulin resistance is associated with changes in Fgf21 DNA methylation in liver of mice. *The Journal of Nutritional Biochemistry* 100: 108907, Doi: 10.1016/J.JNUTBIO.2021.108907.

[2] Krause, C., Britsemmer, J.H., Bernecker, M., Molenaar, A., Taege, N., Geißler, C., et al., 2023. Liver microRNA transcriptome reveals miR-182 as link between type 2 diabetes and fatty liver disease in obesity. *ELife* 12, Doi: 10.7554/ELIFE.92075.